WILEY | Hindawi

Research Article

Performance Sensitivity of a Wind Farm Power Curve Model to Different Signals of the Input Layer of ANNs: Case Studies in the Canary Islands

Sergio Velázquez Medina [ID],[1] José A. Carta,[2] and Ulises Portero Ajenjo[3]

[1]*Department of Electronics and Automatics Engineering, Universidad de Las Palmas de Gran Canaria, Campus de Tafira s/n, 35017 Las Palmas de Gran Canaria, Canary Islands, Spain*
[2]*Department of Mechanical Engineering, University of Las Palmas de Gran Canaria, Campus de Tafira s/n, 35017 Las Palmas de Gran Canaria, Canary Islands, Spain*
[3]*School of Industrial and Civil Engineering, University of Las Palmas de Gran Canaria, Campus de Tafira s/n, 35017 Las Palmas de Gran Canaria, Canary Islands, Spain*

Correspondence should be addressed to Sergio Velázquez Medina; sergio.velazquezmedina@ulpgc.es

Improving the estimation of the power output of a wind farm enables greater integration of this type of energy source in electrical systems. The development of accurate models that represent the real operation of a wind farm is one way to attain this objective. A wind farm power curve model is proposed in this paper which is developed using artificial neural networks, and a study is undertaken of the influence on model performance when parameters such as the meteorological conditions (wind speed and direction) of areas other than the wind farm location are added as signals of the input layer of the neural network. Using such information could be of interest, either to study possible improvements that could be obtained in the performance of the original model, which uses exclusively the meteorological conditions of the area where the wind farm is located, or simply because no reliable meteorological data for the area of the wind farm are available. In the study developed it is deduced that the incorporation of meteorological data from an additional weather station other than that of the wind farm site can improve by up to 17.6% the performance of the original model.

1. Introduction

The power curve of a wind turbine (WT) is a model that relates the electrical power generated by the WT to the wind speed. This characteristic of a WT is of fundamental importance in power output estimation processes. A precise knowledge of the power curve of a WT is vital to optimise the efficiency of these processes and is indispensable for massive wind power integration in electrical systems [1–6].

Manufacturers of WTs provide certified power curve models based on the IEC 61400-12-1 standard [7]. To obtain this certification for the full operating range of the WT within an acceptable period of time, these curves are usually certified using wind simulation systems and not directly at the site where the WT will be definitively located. The power curve of

a WT that is obtained in this way is therefore static. That is to say, it is independent of the actual meteorological conditions of the site where it is to be located, of the surrounding conditions of the terrain (roughness) and of the variations that it may undergo over time or of changes to the operation of the WT due to aging of the system.

Other procedures have been proposed in the literature to establish the power curve models of a WT. These include, for example, polynomial and exponential type parametric models. These define the operating curve of a WT according to various design values including, amongst others, rotor diameter, blade design, start-up speed, rated speed, etc. [8–13]. Carrillo et al. [12] and Lydia et al. [9] reviewed the different types of parametric models defined in the literature, comparing them according to their fit with the power curve

of the manufacturer defined in accordance with IEC 61400-12-1. Carrillo et al. [12] point out in their study that one of the major drawbacks of this type of generic power curve model is the difficulty of confirming that these models are an exact representation of each of the different WT technologies.

Nonparametric models have also been developed to define the power curve of a single WT using artificial intelligence methods [14, 15].

Terrain roughness is one of the factors that most impacts the uncertainty of the energy estimation process of a WT [16, 17]. Terrain roughness additionally needs to be considered according to the direction the wind is coming from [18]. In this respect, in the power curve model development process and for a better estimation of the electrical power of the WT, it is considered important to also take into account wind direction as well as wind speed.

Currently, the integration of wind power in the markets and electrical systems is done through the installation of wind farms (WF) comprised of groups of WTs [19–21]. In these cases, the uncertainty in the estimation of the electrical power of a WT, obtained from the individual power curve model, is increased as a result of the additional wake effect generated between the different WTs in the WF [17, 18, 22–24]. This effect depends on the relative location of each WT with respect to the others, on the predominant wind direction and on the distance between the WTs [18].

This additional uncertainty as a consequence of the integration of a WT in a WF can be corrected through the development of global WF power curve models.

Mingdi You et al. [25] developed a linear power curve of a WT as an integral component of a WF. For development of the individualised model, both wind speed and direction are taken into account. With respect to wind direction, the idea is to divide the spectrum of possible directions into a specific number of ranges, developing a different WT power curve for each of them. Sixteen sectors at most are used, which is equivalent to developing the same model for the data corresponding to a 22.5° range of directions. To estimate the different parameters of the model, these authors used information about the neighbouring WTs. For this reason, according to the authors, the reliability of this model is limited to its use in WFs with a large number of WTs (tens or hundreds).

All the parametric models published in the literature are based exclusively on identifying the power curve of individual WTs.

Marvuglia and Messineo [26] compared three WF power curve models developed on the basis of artificial intelligence techniques. All of these models use the historic wind speed and global power output data of a real WF. They do not consider wind direction as a signal of the input layer.

For estimation of the meteorological conditions of a specific site, studies have been published in the literature in which meteorological data from different areas have been used to optimize the estimation process [27, 28]. For the specific case of the generation of power curve models of WTs or WFs, none of the models found in the literature take into account meteorological conditions (wind speed and direction) of areas other than those of the wind farm. Using

such information could be of interest, either to study possible improvements that could be obtained in the performance of the original model which uses exclusively the meteorological conditions of the area where the wind farm is located, or simply because no reliable meteorological data for the area of the wind farm are available.

The research work undertaken in the present study aims to cover this gap found in the body of knowledge. For this purpose, an adaptive wind farm power curve model (ADWFPC) is proposed using regression techniques based on artificial neural networks (ANNs). The following original studies have been carried out:

(i) A study of the improvements in the model efficiency when meteorological data corresponding to weather stations other than the reference weather station of the wind farm is additionally incorporated in the input layer of the neural network.

(ii) A study of the possibility of using exclusively information from a weather station other than the reference station to generate the adaptive wind farm power curve model.

This case studies the option of generating the power curve model based on real data from other weather stations instead of using estimated meteorological data for the area where the wind farm is situated. Using estimated meteorological data introduces additional uncertainty in the estimation process of the wind farm power output, namely, the uncertainty associated with the model used for the estimation of the meteorological data.

The model was applied to two real WFs located on two islands of the Canary Archipelago (Spain).

2. Materials

The models were generated using real electricity production data of two WFs on two islands of the Canary Archipelago (Spain). The electricity production data corresponded to time instants when all the WTs in the corresponding WF were available for operation.

Wind farm 1 (WF-1) (Figure 1) is located on the east coast of the island of Gran Canaria, very close to the sea and in a flat area with very few natural obstacles in the vicinity. WF-1 has 4 Gamesa G47-660kW wind turbines. These are distributed in two lines virtually perpendicular to the dominant wind direction of the area: the line which connects WT1 with WT2 and the line which joins WT3 with WT4. The distance between WTs in the same line and between lines is 1.6 and 5.5 times the rotor diameter, respectively.

Wind farm 2 (WF-2) (Figure 2) is located inland on Lanzarote island in an area of variable orography. It has 9 Gamesa G52-850 kW wind turbines. Unlike WF-1, all the WTs of WF-2 are practically distributed along a single line (line which connects WT1 with WT9) perpendicular to the dominant wind direction. The distance between the different WTs, measured along that line, is variable, ranging between 2 and 3 times the rotor diameter.

D: Rotor diameter

----Perpendicular to the dominant wind direction.

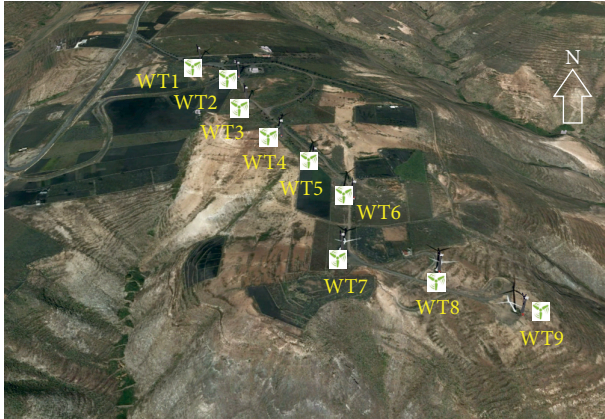FIGURE 1: Distribution of the four wind turbines of WF-1 on Gran Canaria island [29].

FIGURE 2: Distribution of wind turbines of WF-2 on Lanzarote [29].

TABLE 1: Geographic coordinates of the wind turbines.

Code	X(m.)	Y(m.)	Z(m.)
Wind Farm 1			
WF1-WT1	461764	3086314	3
WF1-WT2	461839	3086301	1
WF1-WT3	461681	3086067	5
WF1-WT4	461753	3086038	2
Wind Farm 2			
WF2-WT1	645043	3219819	486
WF2-WT2	645147	3219752	478
WF2-WT3	645186	3219638	473
WF2-WT4	645264	3219548	464
WF2-WT5	645333	3219462	456
WF2-WT6	645403	3219369	448
WF2-WT7	645406	3219213	440
WF2-WT8	645554	3219194	425
WF2-WT9	645664	3219133	405

Tecnológico de Canarias) [30], the Spanish State Meteorological Agency (AEMET, Agencia Española de Meteorología) [31], and the owners of the WFs. The ITC is a public research and development company which pertains to the Canary Government. Among its many lines of research are the analysis of renewable resources and the undertaking of projects such as the wind map of the Canary Islands [32, 33].

Table 2 shows the general data of each of the WSs: the code assigned to each of them, the height above ground level, the geographic coordinates, and the mean annual wind speed for 2008.

Figure 4 shows the distribution of real wind directions for the reference WSs (WS-1 and WS-9) of the WFs.

Table 3 shows the linear correlation coefficients (CC) (1) between the mean hourly wind speeds of the different WSs. The range of CCs obtained is between 0.10 and 0.87. The lowest value was obtained between WS-3 and WS-9. The highest CCs were observed between WS-1 and WS-2 and between WS-2 and WS-7.

$$CC = \frac{\sum_{i=1}^{m} \left(V_{1i} - \overline{V_1} \right) \times \left(V_{2i} - \overline{V_2} \right)}{\sqrt{\sum_{i=1}^{m} \left(V_{1i} - \overline{V_1} \right)^2} \times \sqrt{\sum_{i=1}^{m} \left(V_{2i} - \overline{V_2} \right)^2}} \tag{1}$$

where

CC is Pearson's correlation coefficient between the wind speeds of two weather stations.

V_{1i} and V_{2i} are the wind speed data of the two weather stations for hour "i."

m is the number of data available in the year.

$\overline{V_1}$ and $\overline{V_2}$ are the mean wind speed values for the available data series of the two weather stations.

3. Methodology

3.1. Architecture Used for the Neural Network. The architecture used for the ANNs was comprised of three layers with

As is clear from the above description, and as can be seen in Figures 1 and 2, the two WFs used for this study differ in terms of the distribution pattern of their respective WTs.

Shown in Table 1 are the geographic coordinates of the WTs of the two WFs.

The meteorological data (wind speeds and directions) were recorded at 9 weather stations (WS) installed on four of the seven main islands that make up the Canary Archipelago (Figure 3). These were numbered from WS-1 to WS-9. The reference stations are WS-1 and WS-9 in, respectively, WF-1 and WF-2.

The data used are from 2008 and have a mean hourly frequency.

The meteorological data series were provided by the Technological Institute of the Canary Islands (ITC, Instituto
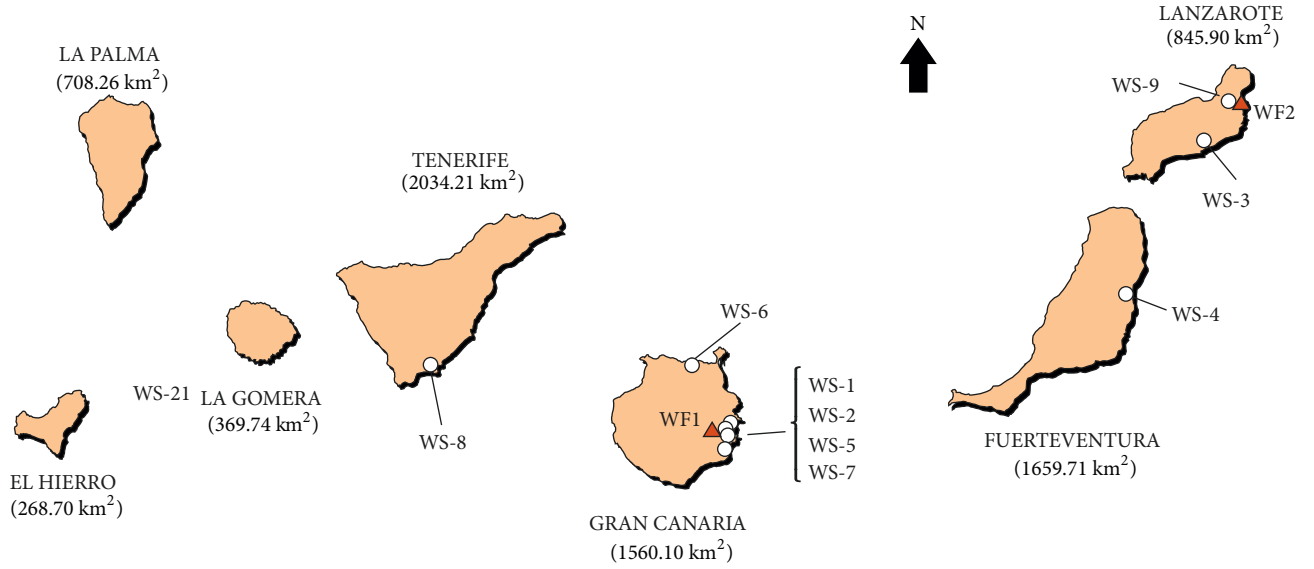
FIGURE 3: Location of the weather stations (WS) and wind farms (WF) used in the study.

TABLE 2: Weather stations used in the study.

Code	Height (m a.g.l.)	X(m.) (north)	Y(m.) (west)	Z(m.) (m.)	Annual mean wind speed(m/s)
WS-1	40	461811	3086432	16	8.3
WS-2	10	461905	3081754	3	7.7
WS-3	10	611130	3147885	24	5.6
WS-4	10	636430	3203469	10	5.4
WS-5	13	461882	3100217	5	6.9
WS-6	10	433517	3111235	472	8.5
WS-7	10	458351	3090136	186	6.0
WS-8	10	345575	3102967″	51	6.0
WS-9	40	645405	3219587	457	8.4

feedforward connections. More specifically, multilayer perceptron topologies (MLPs) were used [34, 35]. This architecture has shown its capacity to satisfactorily approximate any continuous transformation [34, 35] and has been proposed by various authors [36, 37]. A total of 20 neurons were used for the hidden layer. It was verified that model efficiency was not improved with more neurons in this layer. The number of neurons in the input layer varies depending on the case under study. In all the cases considered, the output layer comprised just a single neuron.

The designed architectures were trained using the backpropagation algorithm with sigmoidal activation function [34, 35] and the Levemberg-Marquard method [34, 38] for mean square error minimisation.

The different tests were performed using Matlab software tools for neural networks (the licence was acquired by the Group for Research on Renewable Energy Systems of the University of Las Palmas de Gran Canaria).

3.2. Description of the Study Cases. Figure 5 is a schematic description of the general methodology for generation of ADWFPCs using ANNs. The input layer neurons correspond to the meteorological information (wind speed and/or direction) of one or various WSs. The output layer will have a single neuron which corresponds to the WF power output.

All the available data are divided randomly into three parts to be used in the training, validation and test stages (Figure 5). The proportion of data used for the training, validation, and test stages was 70%, 15%, and 15%, respectively.

The training data subset was used to estimate the weights of the ANN. The validation data subset was used to check the progress of the training of the ANNs, optimizing their parameters. Based on this, and using the data reserved for the test stage, the hourly WF power output is estimated. To assess model precision, a comparison of the data estimated in the test stage with the observed data is undertaken. That is, it constitutes an independent measure of the functioning of the ANN after its training.

TABLE 3: Linear correlation coefficients between the wind speeds recorded at the different weather stations.

	WS-1	WS-2	WS-3	WS-4	WS-5	WS-6	WS-7	WS-8	WS-9
WS-1	1	0.84	0.27	0.34	0.74	0.73	0.77	0.50	0.50
WS-2	0.81	1	0.19	0.25	0.79	0.74	0.87	0.44	0.54
WS-3	0.27	0.19	1	0.70	0.16	0.16	0.18	0.16	0.10
WS-4	0.34	0.25	0.70	1	0.20	0.21	0.22	0.20	0.11
WS-5	0.74	0.79	0.16	0.20	1	0.49	0.78	0.21	0.44
WS-6	0.73	0.74	0.16	0.21	0.49	1	0.61	0.62	0.54
WS-7	0.77	0.87	0.18	0.22	0.78	0.61	1	0.39	0.46
WS-8	0.50	0.44	0.16	0.20	0.21	0.62	0.39	1	0.34
WS-9	0.50	0.54	0.10	0.11	0.44	0.54	0.46	0.34	1

The results obtained were analysed in the present paper for the following cases.

Case 1. This case considers the original model which uses exclusively, as signals of the input layer of the ANN, meteorological data of the reference station of the wind farm. The results obtained in this case were differentiated according to whether only the wind speed data were used, or both the wind speed and wind direction data were used simultaneously (Figure 6(a) vs. Figure 6(b)).

Case 2. Analysis of improvements in the precision of the adaptive model when the data from a WS other than the reference station of the WF is additionally incorporated in the ANN input layer.

Figure 7 shows a schematic representation of the ANN for this case. Unlike the adaptive model of Case 1, this ANN will have an input layer of 4 neurons.

A total of 9 WSs were used in this study (including each reference WS of the two WFs). Each WF reference station was combined with the seven WSs with no connection to either of the two WFs. This means the generation of 7 different models for each of the two WFs.

Case 3. Analysis of the performance of the adaptive model when only the data from a WS other than the reference station of the WF is used in the input layer.

This case was considered because it is possible that there may be no reliable reference station meteorological data available [39]. With this in mind, adaptive models were generated using meteorological data from WSs other than the reference station. The precision of these models was compared with that of the adaptive model obtained following option (b) of Case 1 (Figure 6(b)).

Figure 8 shows a schematic representation of the ANN model for this case. The number of neurons in the different layers is the same as in Case 1, option (b).

3.3. Metrics Used to Compare the Different Models. The metrics defined in (2), (3), and (4) were used to compare the precision of the different models that were generated. These metrics are commonly used in analyses of model efficiency [40–42].

$$\mathrm{MARE} = \frac{1}{n}\sum_{i=1}^{n}\frac{\left|P_i - \hat{P}_i\right|}{P_i}; \quad \begin{cases} P_i > 0 \\ \hat{P}_i > 0 \end{cases} \tag{2}$$

where

MARE is the mean absolute relative error.

P_i is the observed value of the wind farm power output for the time instant i.

$\hat{P}_i$ is the estimated value of the wind farm power output for the time instant i.

n is the number of data used in the test stage.

$$R = \frac{\sum_{i=1}^{n}\left(P_i - \overline{P}\right) \times \left(\hat{P}_i - \overline{\hat{P}}\right)}{\sqrt{\sum_{i=1}^{n}\left(P_i - \overline{P}\right)^2} \times \sqrt{\sum_{i=1}^{n}\left(\hat{P}_i - \overline{\hat{P}}\right)^2}} \tag{3}$$

where

R is Pearson's correlation coefficient between the estimated and observed values of the wind farm power output.

$\overline{P}$ is the mean of the observed values of the power output for the data series of the test stage (Figure 5).

$\overline{\hat{P}}$ is the mean of the estimated values of the power output for the data series of the test stage (Figure 5).

$$I_oA = 1 - \frac{\sum_{i=1}^{n}\left(\hat{P}_i - P_i\right)^2}{\sum_{i=1}^{n}\left(\left|\hat{P}_i - \overline{P}\right| + \left|P_i - \overline{P}\right|\right)^2} \tag{4}$$

where

I_oA (Index of Agreement) evaluates the index of agreement between the values estimated by the model and the observed values of the wind farm power output [40].

4. Results and Discussion

4.1. Discussion of Results for Case 1 (C1). Table 4 shows the results obtained for the different metrics.
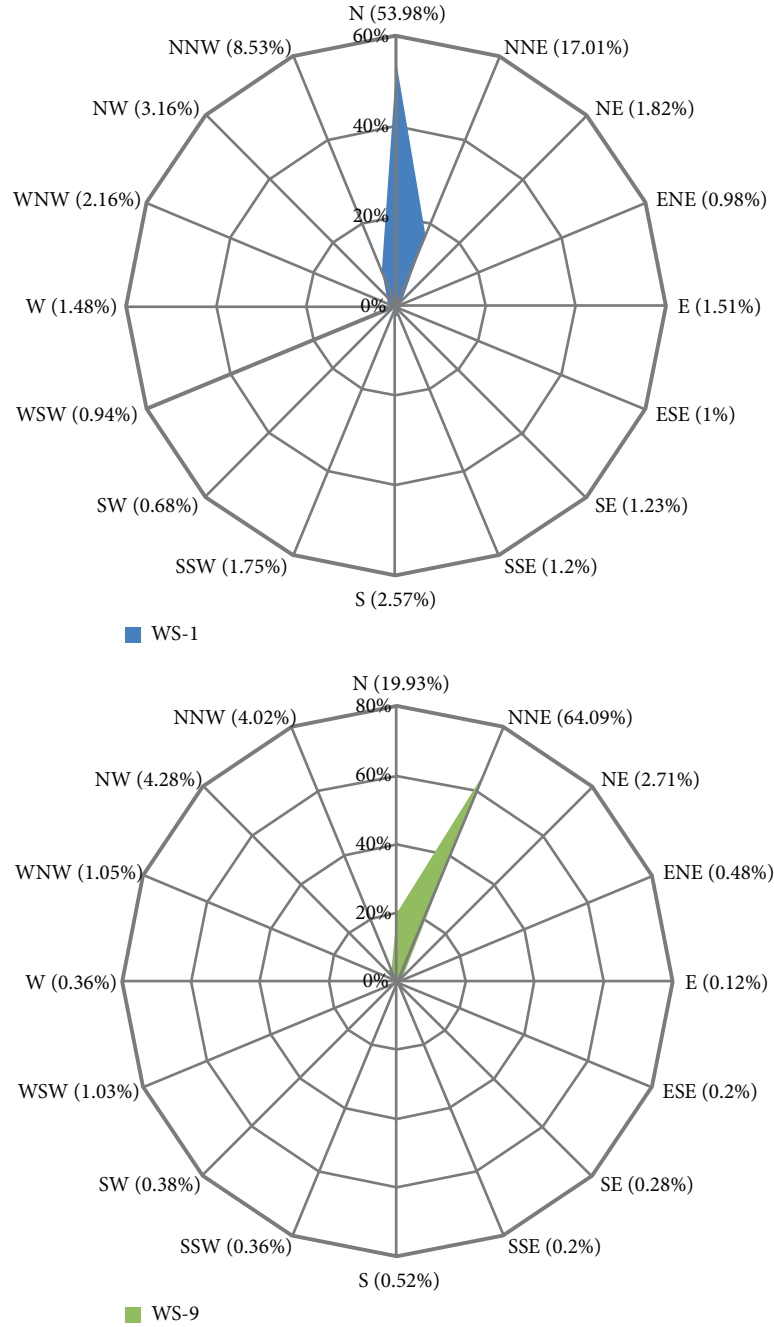
Figure 4: Annual wind direction frequency distribution for WS-1 and WS-9.

Table 4: Comparison of the results of the models generated according to (a) and (b) of Figure 6.

Wind farm	Input layer signal (wind speed)			Input layer signals (wind speed and direction)		
	MARE	R	IoA	MARE	R	IoA
C1-WF-1	0.2492	0.9174	0.9546	0.2438	0.9236	0.9591
C1-WF-2	0.1094	0.9716	0.9855	0.0991	0.9803	0.99

In the simulation of the models generated for the two WFs, it can be seen that the reliability of the model obtained for WF-2 is higher than that for WF-1. This difference in model performance is due to the greater difficulty in the learning stage of WF-1 which has a more complex distribution of WTs on the ground: there are various lines of WTs and the distances are relatively small, both between WTs on the same line and between lines.

Another of the conclusions that can be drawn from the data shown in Table 4 is that, when incorporating wind direction in the input layer of the ANN, the new models that
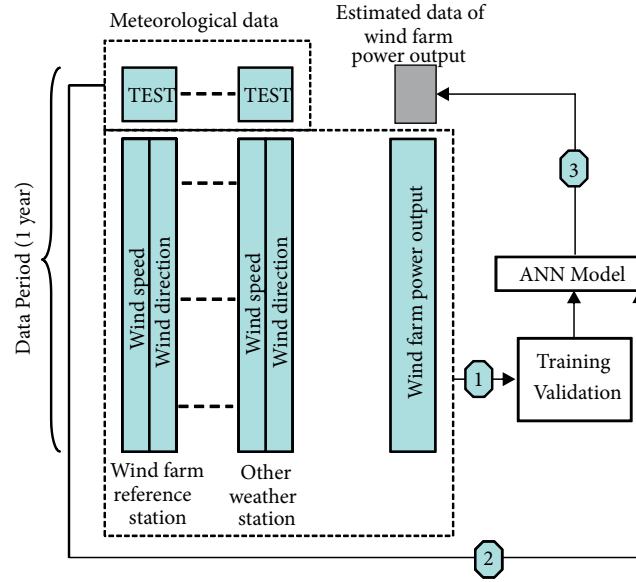
FIGURE 5: General layout of the methodology followed to obtain the adaptive wind farm power curves.
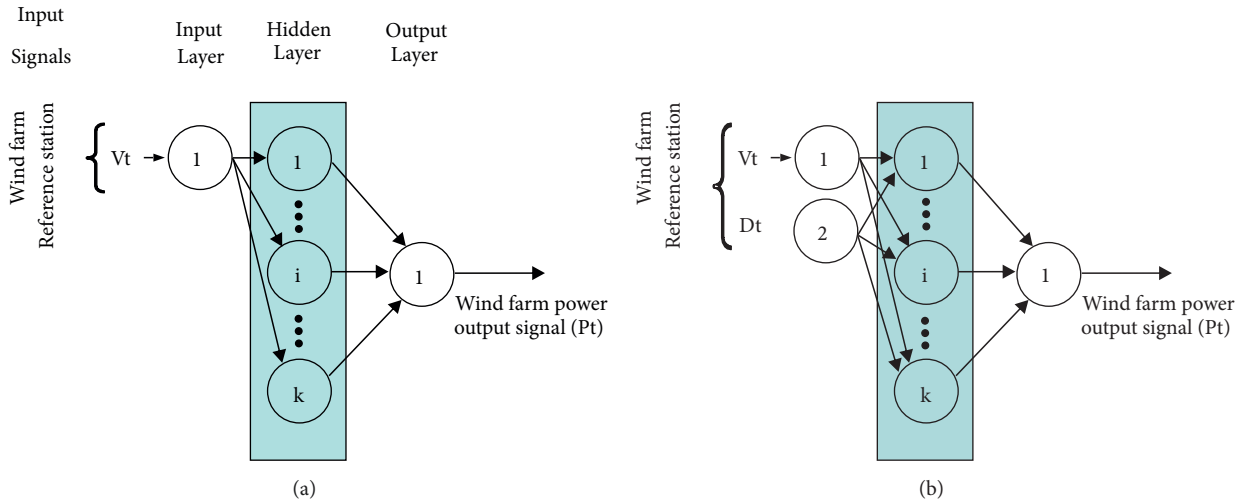

(a)

(b)

FIGURE 6: Schematic representation of the ANNs of the ADWFPC model when only wind speed is used in the input layer (option (a)) vs. when wind speed and direction are used (option (b)).

are generated for the WFs perform better than the original model. It can also be seen that the degree of improvement differs depending on whether the new model is applied to WF-1 or WF-2. For WF-1, and in relation to the MARE metric, a 2.2% improvement is found and for WF-2 the improvement is 4.3 times greater (9.4%).

4.2. Discussion of the Results for Case 2 (C2). The different simulations analysed in Case 2 were coded as shown in Table 5. The simulations coded as "C2-WF1 S0" and "C2-WF2 S0" correspond to the adaptive models obtained according to Case 1 (Figure 6(b)). These were compared with the remaining simulations, the wind farm power curve models which were obtained according to Case 2 (Figure 7).

Figures 9 and 10 show, respectively, the "MARE" and correlation coefficient "R" results obtained when applying the different models. For WF-1, it can be seen that the results obtained with the models developed for all the simulations of Case 2 were better than those obtained according to Case 1, option (b) (Table 4). The degree of improvement is independent of the correlation coefficient (Table 3) that exists between the reference WS of the WF and the additional WS. That is, a better value for the correlation coefficient does not directly imply a better degree of improvement. An example of this can be seen by comparing the results of the simulations C2-WF1 S3 and C2-WF1 S6.

For WF-2, the results obtained initially for Simulation 0 are already quite good, with a "MARE" below 0.1 and an IoA of 0.99. Even so, some of the models developed according
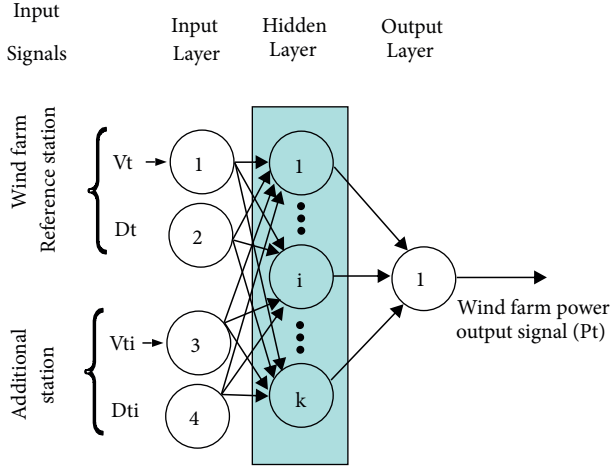
FIGURE 7: Schematic representation of the ANN of the ADWFPC model when the wind speed and direction data of a station other than the reference station of the wind farm are additionally incorporated.
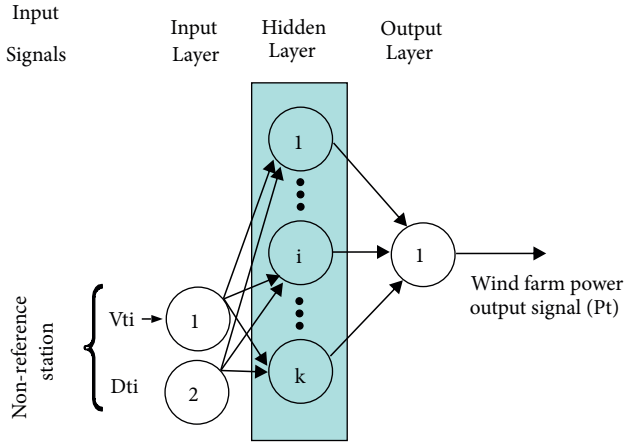

FIGURE 8: Schematic representation of the ANN used to generate the ADWFPC model when only using in the input layer the wind speed and direction of a WS other than the reference station of the WF.

TABLE 5: Simulations studied in Case 2.

Simulations for WF1	Simulations for WF2	Additional WS
C2-WF1 S0	C2-WF2 S0	None
C2-WF1 S1	C2-WF2 S1	WS-2
C2-WF1 S2	C2-WF2 S2	WS-3
C2-WF1 S3	C2-WF2 S3	WS-4
C2-WF1 S4	C2-WF2 S4	WS-5
C2-WF1 S5	C2-WF2 S5	WS-6
C2-WF1 S6	C2-WF2 S6	WS-7
C2-WF1 S7	C2-WF2 S7	WS-8

the meteorological data of a WS other than the reference stations. A total of 7 models were therefore obtained for each WF. Model performance according to Case 3 was then compared with that of the adaptive model obtained according to Case 1, option (b) (Figure 6(b)). For this purpose, the ratio was calculated between the IoA obtained for each of the models of Case 3 (C3-IoA) and that obtained for each of the models of Case 1 (C1-IoA). The results are shown in Figure 12. Represented on the x-axis is the CC between the WS used to generate the model other than the reference WSs and the actual reference WS of the WF.

It can be seen that the higher the CC the greater the degree of similarity between the ADWFPC models obtained according to Cases 1 and 3. For CC values above 0.7, the degree of similarity, expressed as the ratio between the IoAs, is above 0.9.

5. Conclusions

From the study undertaken in the present paper it can be deduced that when the meteorological data from an additional weather station other than the reference station of the wind farm (Case 2 of this study) are incorporated in the input layer of the neural network, the model performance can improve the results obtained for the original model (Case 1). For WF-1, model performance increased in 100% of the cases. It was also observed that the degree of improvement is independent of the correlation coefficient (CC) between the corresponding reference weather station of the wind farm and the additional weather station.

The conclusions obtained from the comparison of the models developed according to Cases 1 and 2 can serve as a reference for optimization of the performance of already developed power curve models in which only data from the reference weather station of the wind farm are used.

When the meteorological data from a weather station other than the reference station were used instead of the data of the actual reference station of the wind farm in the input layer of the ANN (Case 3), the degree of similarity between the results of the adaptive model obtained in this way and the results obtained with the adaptive model according to Case 1, option (b) (Figure 6(b)), increases with the CC between the wind speeds of the reference station and the nonreference station. For a CC over 0.7, the degree of similarity between the adaptive models obtained according to Cases 1 and 3 was
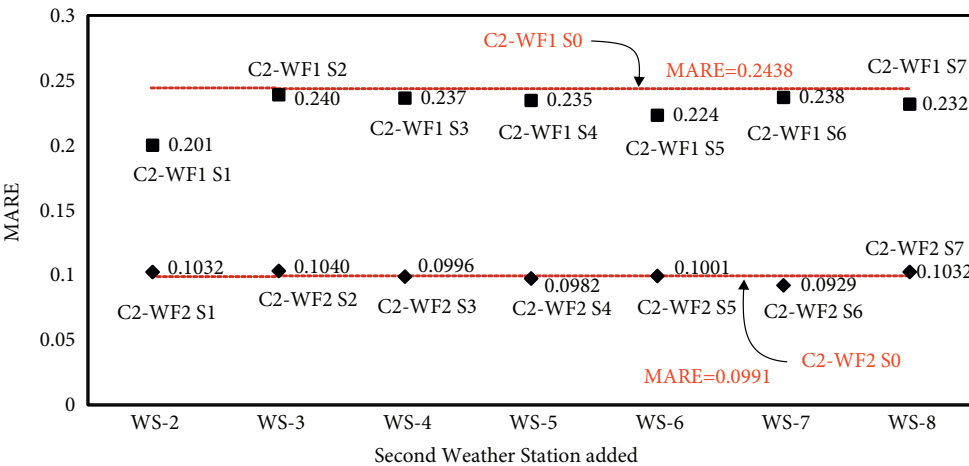
to Case 2 improved on the initial result. More specifically, the "MARE" and "R" results with the Case 2 models for the C2-WF2 S4 and the C2-WF2 S6 were better than those obtained with the Case 1 models, option (b). As with WF-1, it is concluded that the degree of improvement in model efficiency is independent of the CC that exists between the reference WS of the WF and the additional WS.

Figure 11 shows the results obtained for "IoA" (4). The results follow the same general pattern seen for "MARE" and "R." That is, for the case of WF-1, the results obtained with all the models of Case 2 were better than the initial result obtained with a single station (C2-WF1 S0). Similarly, it can be seen for WF-2 that the results obtained for C2-WF2 S4 and C2-WF2 S6 were better than the initial result.

4.3. Discussion of the Results for Case 3. For Case 3 and for each of the WFs, the adaptive models were generated using

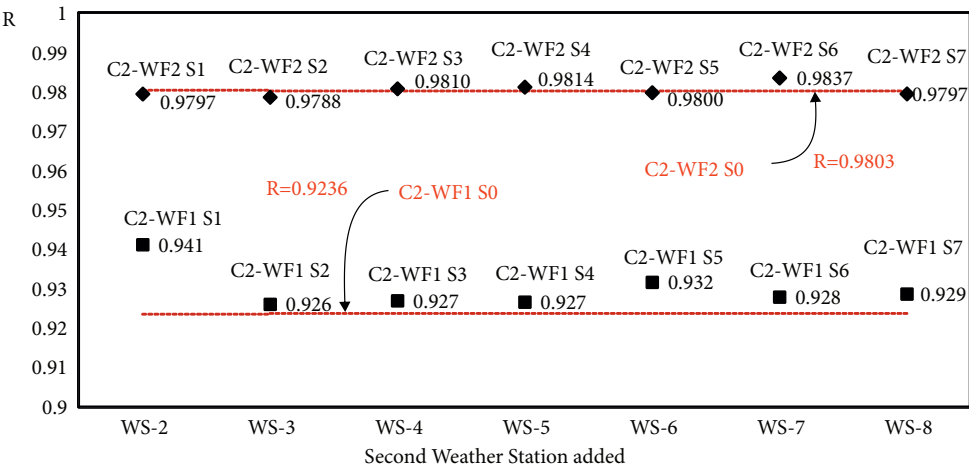FIGURE 9: Comparison of the "MARE" results for Case 2 and Case 1 (C2-WF S0).

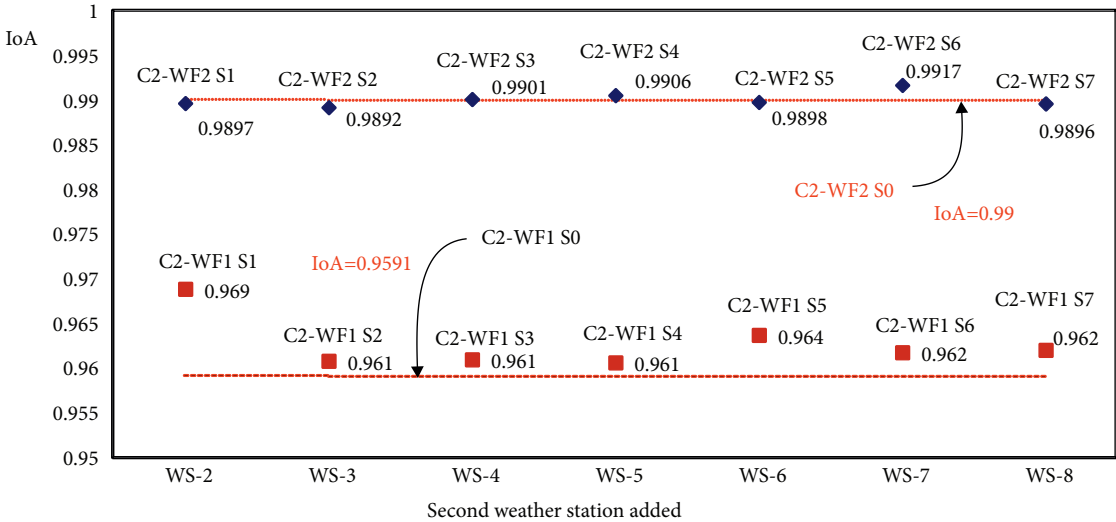FIGURE 10: Comparison of the "R" results for Case 2 and Case 1 (C2-WF S0).

FIGURE 11: Comparison of the "IoA" results for Case 2 and Case 1 (C2-WF S0).
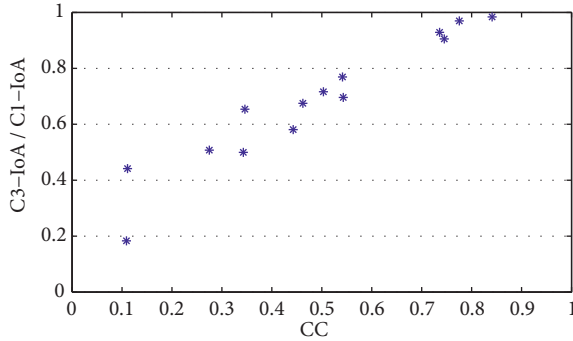
Figure 12: Comparison of the precision of the adaptive models calculated according to Cases 1 and 3.

above 0.9 (Figure 12). In this respect, it is possible to know the additional uncertainty when the power curve model is generated with data other than the data of the reference weather station of the wind farm.

Nomenclature

ANN:	Artificial neural network
CC:	Pearson's correlation coefficient between the wind speeds of different weather stations
IoA:	Index of Agreement
MARE:	Mean absolute relative error
ADWFPC:	Adaptive wind farm power curve
R:	Pearson's correlation coefficient between the estimated and observed values of the electrical power of a wind farm
WF-1:	Wind farm 1
WF-2:	Wind farm 2
WS:	Weather station
WT:	Wind turbine.

Data Availability

The wind farms data used to support the findings of this study were supplied by the owners under confidential terms and conditions and so cannot be made freely available. Requests for access to these data should be made to the following: Wind farm 1: Owner: Soslaires Canarias, S.L. (https://empresite.eleconomista.es/SOSLAIRES-CANARIAS.html) Wind farm 2: Owner: Eólicas de Lanzarote, S.L. (https://empresite.eleconomista.es/EOLICAS-LANZAROTE.html). The meteorological data used to support the findings of this study are available from the corresponding author upon request.

Disclosure

No funding sources had any influence on study design, collection, analysis, or interpretation of data, manuscript preparation, or the decision to submit for publication.

Conflicts of Interest

The authors declare that there are no conflicts of interest.

Acknowledgments

References

[1] A. V. Ntomaris and A. G. Bakirtzis, "Stochastic scheduling of hybrid power stations in insular power systems with high wind penetration," *IEEE Transactions on Power Systems*, vol. 31, no. 5, pp. 3424–3436, 2016.

[2] D. Dhungana and R. Karki, "Data constrained adequacy assessment for wind resource planning," *IEEE Transactions on Sustainable Energy*, vol. 6, no. 1, pp. 219–227, 2015.

[3] Y. Kuang, Y. Zhang, B. Zhou et al., "A review of renewable energy utilization in islands," *Renewable & Sustainable Energy Reviews*, vol. 59, pp. 504–513, 2016.

[4] U. Portero, S. Velázquez, and J. A. Carta, "Sizing of a wind-hydro system using a reversible hydraulic facility with seawater. A case study in the Canary Islands," *Energy Conversion and Management*, vol. 106, pp. 1251–1263, 2015.

[5] S. Wang, X. Zhang, L. Ge, and L. Wu, "2-D wind speed statistical model for reliability assessment of microgrid," *IEEE Transactions on Sustainable Energy*, vol. 7, no. 3, pp. 1159–1169, 2016.

[6] I. González-Aparicio and A. Zucker, "Impact of wind power uncertainty forecasting on the market integration of wind energy in Spain," *Applied Energy*, vol. 159, pp. 334–349, 2015.

[7] International Electrotechnical Comission (IEC), "Power performance measurements of electricity producing wind turbines," IEC 61400-12-1, 2005.

[8] G. Bai, B. Fleck, and M. J. Zuo, "A stochastic power curve for wind turbines with reduced variability using conditional copula," *Wind Energy*, vol. 19, no. 8, pp. 1519–1534, 2016.

[9] M. Lydia, S. S. Kumar, A. I. Selvakumar, and G. E. Prem Kumar, "A comprehensive review on wind turbine power curve modeling techniques," *Renewable & Sustainable Energy Reviews*, vol. 30, pp. 452–460, 2014.

[10] A. Feijóo and D. Villanueva, "Wind farm power distribution function considering wake effects," *IEEE Transactions on Power Systems*, vol. 32, no. 4, pp. 3313-3314, 2017.

[11] A. Feijóo and D. Villanueva, "Four-parameter models for wind farm power curves andpower probability density functions," *IEEE Transactions on Sustainable Energy*, vol. 8, no. 4, pp. 1783-1784, 2017.

[12] C. Carrillo, A. F. Obando Montaño, J. Cidrás, and E. Díaz-Dorado, "Review of power curve modelling for wind turbines," *Renewable & Sustainable Energy Reviews*, vol. 21, pp. 572–581, 2013.

[13] D. Villanueva and A. Feijóo, "Normal-based model for true power curves of wind turbines," *IEEE Transactions on Sustainable Energy*, vol. 7, no. 3, pp. 1005–1011, 2016.

[14] F. Pelletier, C. Masson, and A. Tahan, "Wind turbine power curve modelling using artificial neural network," *Journal of Renewable Energy*, vol. 89, pp. 207–214, 2016.

[15] T. Ouyang, A. Kusiak, and Y. He, "Modeling wind-turbine power curve: a data partitioning and mining approach," *Journal of Renewable Energy*, vol. 102, pp. 1–8, 2017.

[16] S. Jung, O. A. Vanli, and S.-D. Kwon, "Wind energy potential assessment considering the uncertainties due to limited data," *Applied Energy*, vol. 102, pp. 1492–1503, 2013.

[17] L. Wang, A. C. Tan, M. Cholette, and Y. Gu, "Comparison of the effectiveness of analytical wake models for wind farm with constant and variable hub heights," *Energy Conversion and Management*, vol. 124, pp. 189–202, 2016.

[18] S. Grassi, S. Junghans, and M. Raubal, "Assessment of the wake effect on the energy production of onshore wind farms using GIS," *Applied Energy*, vol. 136, pp. 827–837, 2014.

[19] L. Martínez-Villaseñor, H. Ponce, J. A. Marmolejo-Saucedo, J. M. Ramírez, and A. Hernández, "Analysis of constraint-handling in metaheuristic approaches for the generation and transmission expansion planning problem with renewable energy," *Complexity*, vol. 2018, Article ID 1438196, 22 pages, 2018.

[20] M. Deissenroth, M. Klein, K. Nienhaus, and M. Reeg, "Assessing the plurality of actors and policy interactions: agent-based modelling of renewable energy market integration," *Complexity*, vol. 2017, Article ID 7494313, 24 pages, 2017.

[21] J. M. Torres and R. M. Aguilar, "Using deep learning to predict complex systems: a case study in wind farm generation," *Complexity*, vol. 2018, Article ID 9327536, 10 pages, 2018.

[22] H. Jadhav and R. Roy, "Effect of turbine wake on optimal generation schedule and transmission losses in wind integrated power system," *Sustainable Energy Technologies and Assessments*, vol. 7, pp. 123–135, 2014.

[23] S. Pookpunt and W. Ongsakul, "Design of optimal wind farm configuration using a binary particle swarm optimization at Huasai district, Southern Thailand," *Energy Conversion and Management*, vol. 108, pp. 160–180, 2016.

[24] L. Wang, A. C. Tan, M. E. Cholette, and Y. Gu, "Optimization of wind farm layout with complex land divisions," *Journal of Renewable Energy*, vol. 105, pp. 30–40, 2017.

[25] M. You, B. Liu, E. Byon, S. Huang, and J. Jin, "Direction-dependent power curve modeling for multiple interacting wind turbines," *IEEE Transactions on Power Systems*, vol. 33, no. 2, pp. 1725–1733, 2018.

[26] A. Marvuglia and A. Messineo, "Monitoring of wind farms' power curves using machine learning techniques," *Applied Energy*, vol. 98, pp. 574–583, 2012.

[27] J. A. Carta, S. Velázquez, and P. Cabrera, "A review of measure-correlate-predict (MCP) methods used to estimate long-term wind characteristics at a target site," *Renewable & Sustainable Energy Reviews*, vol. 27, pp. 362–400, 2013.

[28] J. A. Carta, P. Cabrera, J. M. Matías, and F. Castellano, "Comparison of feature selection methods using ANNs in MCP-wind speed methods. A case study," *Applied Energy*, vol. 158, pp. 490–507, 2015.

[29] Canary Government, "Sistema de información territorial de Canarias (IDECanarias)" (Spanish), 2018, http://visor.grafcan.es/visorweb/.

[30] Canary Government, "Technological institute of the Canary Islands (ITC - Instituto Tecnológico de Canarias)," 2018, http://www.itccanarias.org/web/.

[31] Spanish Government, "Spanish state meteorological agency (AEMET - Agencia Española de Meteorología)," 2018, http://www.aemet.es/es/en.

[32] Technological Institute of the Canary Islands (ITC - Instituto Tecnológico de Canarias), "Valoración de recursos energéticos renovables" (Spanish), 2018, http://www.itccanarias.org/web/actividades/eerr/recursos_energeticos.jsp?lang=en.

[33] Technological Institute of the Canary Islands (ITC - Instituto Tecnológico de Canarias), "Recurso Eólico de Canarias" (Spanish), 2018, http://www.itccanarias.org/recursoeolico/.

[34] J. C. Principe, N. R. Euliano, and W. C. Lefebvre, "Neural and adaptive systems," in *Fundamentals through Simulations*, John Wiley & Sons, Inc., New York, NY, USA, 1st edition, 2000.

[35] T. Masters, *Practical Neural Network Recipes in C++*, Morgan Kaufmann Publishers, Calif, USA, 1st edition, 1993.

[36] A. Oztopal, "Artificial neural network approach to spatial estimation of wind velocity," *Energy Conversion and Management*, vol. 47, pp. 395–406, 2006.

[37] M. Monfared, H. Rastegar, and H. M. Kojabadi, "A new strategy for wind speed forecasting using artificial intelligent methods," *Journal of Renewable Energy*, vol. 34, no. 3, pp. 845–848, 2009.

[38] N. R. Draper and H. Smith, *Applied Regression Analysis*, John Wiley & Sons, Inc, 1966.

[39] Y. Zhao, L. Ye, W. Wang, H. Sun, Y. Ju, and Y. Tang, "Data-driven correction approach to refine power curve of wind farm under wind curtailment," *IEEE Transactions on Sustainable Energy*, vol. 9, no. 1, pp. 95–105, 2018.

[40] C. J. Willmott, S. M. Robeson, and K. Matsuura, "A refined index of model performance," *International Journal of Climatology*, vol. 32, no. 13, pp. 2088–2094, 2012.

[41] P. Brandimarte, *Quantitative Methods: An Introduction for Business Management*, Wiley, NJ, USA, 1st edition, 2011.

[42] D. S. Wilks, *Statistical Methods in the Atmospheric Sciences*, Academic Press, USA, 3rd edition, 2011.